

Muon g-2 anomaly and extra interaction of composite Higgs in a dynamically broken electroweak theory

B.A. Arbuzov

*Skobeltsyn Institute for Nuclear Physics, Moscow State University
119899 Moscow, Russia*

In electroweak theory without elementary Higgs scalars existence of a solution, which breaks initial symmetry is shown. A composite scalar doublet serves as a substitute for usual Higgs. The mass of the surviving Higgs scalar is predicted to be $M_H = 117 \pm 7 \text{ GeV}$. The resulting theory contains realistic W, Z, t masses and composite massive Higgs. Parameters used are g, θ_W , cut-off $\Lambda \simeq 3500 \text{ GeV}$ and triple gauge constant $\lambda_V \simeq -0.034$. Stable nontrivial solution for extra interactions of the Higgs particle gives contribution to muon $g - 2$: $\Delta a = 49.4 \cdot 10^{-10}$ that agrees with the recently reported anomaly. The extra interaction leads to a number of experimental consequences for B.R. of Higgs decay and its production cross-sections in e^+e^- and $\bar{p}p$ collisions including recommendation for looking for Higgs via decay $H \rightarrow 2\gamma$.

1 Introduction

The widely popular Higgs mechanism [1] of the electroweak symmetry breaking needs initial scalar fields, which look rather less attractive, than the well-known gauge interactions of vector and spinor fields. Experimental facilities now approach the region of possible discovery of the Higgs. There are even indications in favour of the Higgs mass $M_H = 115^{+1.3}_{-0.9} \text{ GeV}$ [2]. In view of these considerations it may be useful to study once more possibilities, which differ from the standard Higgs mechanism and to look for experimental consequences of these possibilities. On the other hand there are serious indications on a discrepancy with theoretical values in measurements of the muon anomalous magnetic moment [3].

In the present work¹ we consider a model, which might serve a substitute for the Standard Model in respect to symmetry breaking. The model leads to a number of effects, which differ from SM results, in particular, it gives reasonable effect for the muon $g - 2$.

We are basing here on the proposal, which was done in works [4], [5], the main point of which consists in application of N.N. Bogolyubov method of quasi-averages [6] to a simple model. Let us summarize the essence of the approach [4] with some necessary corrections. Namely we consider $U(1)$ massless gauge field A_μ and also massless spinor field ψ , which interact in the following way

$$\begin{aligned} L = & \frac{i}{2}(\bar{\psi}\gamma_\rho\partial_\rho\psi - \partial_\rho\bar{\psi}\gamma_\rho\psi) - \frac{1}{4}A_{\mu\nu}A_{\mu\nu} + \\ & + e_L\bar{\psi}_L\gamma_\rho\psi_LA_\rho + e_R\bar{\psi}_R\gamma_\rho\psi_RA_\rho; \\ A_{\mu\nu} = & \partial_\mu A_\nu - \partial_\nu A_\mu; \end{aligned} \quad (1)$$

where as usually

$$\psi_L = \frac{1+\gamma_5}{2}\psi; \quad \psi_R = \frac{1-\gamma_5}{2}\psi.$$

We will not discuss here the problem of the triangle axial anomaly, bearing in mind that in a more realistic model one always can arrange cancellation of the anomalies by a suitable choice of fermions' charges, in the same way as it occurs in the Standard Model.

Now we start to apply Bogolyubov quasi-averages method [6]². In view of looking for symmetry breaking we add to (1) additional term

$$\epsilon \cdot \bar{\psi}_L\psi_R\bar{\psi}_R\psi_L. \quad (2)$$

Now let us consider the theory with $\epsilon \neq 0$, calculate necessary quantities (averages) and only at this stage take limit $\epsilon \rightarrow 0$. In this limit, according [6], we come to quasi-averages, which not always coincide with the corresponding averages, which one obtains directly from the initial Lagrangian (1).

¹The work is supported in part by grants "Universities of Russia" 015.02.02.05 (990588) and RFBR 01-02-16209.

²The quasi-averages method was first applied to quantum field theory problems in work [7].

$$\begin{array}{ccc} \text{Diagram} & = & \Delta L_x; \quad \text{Diagram} & = & \Delta L_y; \quad \text{Diagram} & = & \Delta L_z. \end{array}$$

$$\begin{array}{c} \text{Diagram} = \text{Diagram} + \text{Diagram} + \text{Diagram} + \\ \epsilon \end{array} + \begin{array}{c} \text{Diagram} \\ + \\ \text{Diagram} \\ + \\ \text{Diagram} \\ + \\ \text{Diagram} \end{array} + \begin{array}{c} \text{Diagram} \\ + \\ \text{Diagram} \\ + \\ \text{Diagram} \\ + \\ \text{Diagram} \end{array} + \begin{array}{c} \text{Diagram} \\ + \\ \text{Diagram} \\ + \\ \text{Diagram} \\ + \\ \text{Diagram} \end{array}$$

(a)

$$\begin{array}{c} \text{Diagram} + \text{Diagram} = \text{Diagram} + \text{Diagram} + \\ + \text{Diagram} + \text{Diagram} + \text{Diagram} + \text{Diagram} + \\ + \text{Diagram} + \text{Diagram} + \text{Diagram} + \text{Diagram} + \\ + \text{Diagram} + \text{Diagram} + \text{Diagram} + \text{Diagram} + \\ + \text{Diagram} + \text{Diagram} + \text{Diagram} + \text{Diagram} \end{array}$$

(b)

Figure 1. Diagrams for Eq. (4). Thick lines represent left spinors ψ_L and thin lines represent right ones ψ_R ; (a) corresponds to the first equation of set (4) and (b) corresponds to the second equation of (4). The third equation follows from (b) by mutual exchange thick \leftrightarrow thin

Because of additional term (2) the following additional effective terms in Lagrangian (1) inevitably appear

$$\begin{aligned}\Delta L_x &= x \cdot \bar{\psi}_L \gamma_\rho \psi_L \bar{\psi}_R \gamma_\rho \psi_R; & \Delta L_y &= \frac{y}{2} \cdot \bar{\psi}_L \gamma_\rho \psi_L \bar{\psi}_L \gamma_\rho \psi_L; \\ \Delta L_z &= \frac{z}{2} \cdot \bar{\psi}_R \gamma_\rho \psi_R \bar{\psi}_R \gamma_\rho \psi_R.\end{aligned}\quad (3)$$

The corresponding vertices should have form-factors, which define effective cut-off Λ . The origin of the cut-off is connected with self-consistent solution of the corresponding dynamical equations. A realization of this mechanism will be shown below in Appendix. In the present work we just set upper limit at Euclidean $p^2 = \Lambda^2$ in momentum integrals.

We consider compensation equations [6, 8] (in other words, gap equations) for x, y, z in one-loop approximation (see Fig. 1). These equations are taken in the method of Fradkin full-vertices expansion [9]. The applicability of the method can be verified provided terms with more loops give much smaller contribution, than the first approximation does. We use here free lines, because one-loop terms give zero main contributions to fermion propagators. For the moment we neglect gauge field A_μ exchange loops, and obtain following set of equations

$$\begin{aligned}x &= -\frac{\epsilon}{2} + \frac{\Lambda^2}{16\pi^2}(-3x^2 - 2x(y+z)); \\ y &= \frac{\Lambda^2}{16\pi^2}(-x^2); & z &= \frac{\Lambda^2}{16\pi^2}(-x^2);\end{aligned}\quad (4)$$

Let X, Y, Z be dimensionless variables

$$X = x \frac{\Lambda^2}{16\pi^2}; \quad Y = y \frac{\Lambda^2}{16\pi^2}; \quad Z = z \frac{\Lambda^2}{16\pi^2}; \quad (5)$$

Let us look for solutions of set (4). At this stage we also set $\epsilon \rightarrow 0$. There is, of course, trivial solution $x = y = z = 0$. In addition we have two nontrivial solutions.

$$Z_1 = Y_1 = -1; \quad X_1 = 1; \quad (6)$$

$$Z_2 = Y_2 = -\frac{1}{16}; \quad X_2 = -\frac{1}{4}. \quad (7)$$

As we shall see further, just the second solution (7) will be the most interesting.

Now let us consider scalar bound states $(\bar{\psi}_L \psi_R, \bar{\psi}_R \psi_L)$.

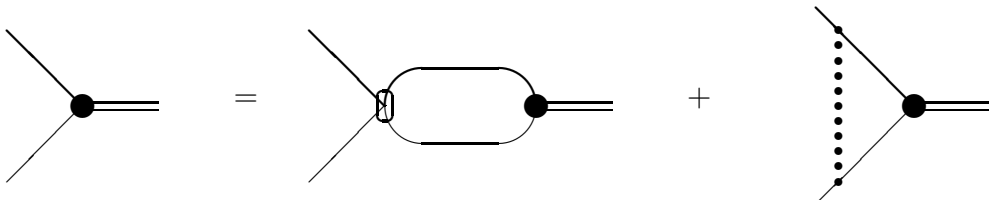


Figure 2. Diagram representation of Bethe-Salpeter equation for scalar bound states. Dotted line represents gauge vector field.

Without e^2 corrections we have from Bethe-Salpeter equation in one-loop approximation (see Fig. 2)

$$\begin{aligned} G &= -4X F(\xi) G; \quad \xi = \frac{k^2}{4\Lambda^2}; \quad \mu = \frac{m^2}{\Lambda^2}; \\ F(\xi) &= 1 - \frac{5}{2}\xi + 2\xi \log \frac{4\xi}{1+\xi}; \quad \mu \ll \xi < 1; \\ F(\xi) &= 1 + \frac{1}{3}\xi + 2\xi \log \mu + O(\xi\mu, \xi^2); \quad \xi \leq \mu. \end{aligned} \quad (8)$$

where $G = \text{const}$ is just the Bethe-Salpeter wave function. Here m means a fermion mass, which will be shown to be nonzero, and k^2 is the scalar state Euclidean momentum squared, that is $k^2 > 0$ means tachyon mass of the scalar. Function $F(\xi)$ decreases from the value $F(0) = 1$ with ξ increasing. We see, that for solution (7) we have bound state with $k^2 = 0$ in full correspondence with Bogolyubov-Goldstone theorem [8], [10]. As for the first solution (6), there is no solution of Eq. (8) at all. So we have to concentrate our attention on the solution (7). Note, that there is an additional argument in favour of solution (7). Namely, values X and especially Y, Z are small enough, so we may expect, that many-loop terms will not influence results strongly.

Now let us take into account vector boson corrections. Equation for the bound state (8) is modified due to two sources. The first one corresponds to vector boson exchange loops in set (4). Here corrections appear, for example, of such form

$$\frac{6e_L e_R x}{16\pi^2} \log \frac{\Lambda^2}{p^2}.$$

Here p is the momentum of integration in Eq. (8). In the present note we will restrict ourselves by main logarithmic approximation, in which such terms do not contribute to results. Indeed, due to simple relation

$$\int_0^{\Lambda^2} x^n \log \frac{\Lambda^2}{x} dx = \frac{(\Lambda^2)^{n+1}}{(n+1)^2}; \quad (9)$$

there is no logarithms in final expressions. So the only important contribution consists in loop e^2 corrections to Eq. (8). In Landau gauge there is only one such contribution: the triangle diagram. We draw at Fig. 2 only this diagram, but the gauge invariance of the result is checked by direct calculations in an arbitrary gauge. So we now have

$$G = F(\xi) G + \frac{3e_L e_R}{16\pi^2} \log \frac{\Lambda^2}{m^2} G. \quad (10)$$

We see, that for small e_L, e_R possible eigenvalues ξ are also small. Then we have following condition for an eigenvalue

$$F(\xi) + \frac{3e_L e_R}{16\pi^2} \log \frac{\Lambda^2}{m^2} = 1; \quad (11)$$

We see, that there is tachyon bound state in case e^2 contribution being positive. Really, the eigenvalue condition for small e_i^2 reads

$$k^2 = m_0^2 = \frac{3e_L e_R}{8\pi^2} \Lambda^2. \quad (12)$$

The result corresponds to main logarithmic approximation. Thus provided $(e_L e_R) > 0$ we have scalar complex tachyon ϕ with negative mass squared $-m_0^2$.

We have the following vertices of interaction of ϕ with spinors

$$G \left(\bar{\psi}_R \psi_L \phi + \bar{\psi}_L \psi_R \phi^* \right). \quad (13)$$

Normalization condition of Bethe-Salpeter equation gives

$$G^2 = \frac{16 \pi^2}{\log(\Lambda^2/m^2)}. \quad (14)$$

Then we calculate box diagram with four scalar legs. This gives us effective constant λ , which enters into additional term

$$\Delta L = -\lambda (\phi^* \phi) (\phi^* \phi); \quad \lambda = \frac{G^4}{16 \pi^2} \log(\Lambda^2/m^2). \quad (15)$$

Now we come to the usual Higgs model [1] with m_0^2 (12), λ (15) and ϕ charge $e_L - e_R$.

Thus from expressions (12, 15) we have usual vacuum average of $\sqrt{2} \operatorname{Re} \phi = \eta$

$$\eta^2 = \frac{m_0^2}{\lambda} = \frac{3 e_L e_R}{128 \pi^4} \Lambda^2 \log \frac{\Lambda^2}{m^2}. \quad (16)$$

The vector boson mass duly arises and it reads as follows

$$M^2 = \frac{3 (e_L - e_R)^2 e_L e_R}{128 \pi^4} \Lambda^2 \log \frac{\Lambda^2}{m^2}. \quad (17)$$

Interaction (13) leads to spinor mass m

$$m = \frac{G \eta}{\sqrt{2}}; \quad m^2 = \frac{3 e_L e_R}{8 \pi^2} \Lambda^2. \quad (18)$$

Thus, we obtain the result, that initially massless model of interaction of a spinor with a vector becomes after the symmetry breaking just a close analog of the Higgs model. We have now vector boson mass (17), spinor mass (18) and a scalar bound state with mass $\sqrt{2} m_0$,

$$m_H^2 = 2 m_0^2 = \frac{3 e_L e_R}{4 \pi^2} \Lambda^2. \quad (19)$$

We would formulate qualitative result of the simple model study as follows: in the massless model with Lagrangian (1) with $(e_L \cdot e_R) > 0$ there arises fermion-antifermion condensate, which defines masses M , m , M_H according to (17, 18, 19).

Note, that variants of dynamical breaking of the electroweak symmetry without elementary scalars were considered in various aspects (see, e.g. paper [11]). The possibility of scalars being composed of fundamental spinors was considered e.g. in well-known paper [12].

2 Realistic model in the leading order of $1/N_c$ expansion

Here we will proceed in the same line, but choose more realistic model, including one coloured left doublet $\psi_L = (t_L, b_L)$ and two right singlets t_R, b_R , which simulate the heaviest quark pair. They interact with $SU(2) \times U(1)$ gauge bosons in standard way, so that the initial Lagrangian corresponds to the Standard Model with one heavy quark (initially massless) generation without Higgs sector and looks like

$$\begin{aligned}
L = & \frac{i}{2}(\bar{\psi}_L \gamma_\rho \partial_\rho \psi_L - \partial_\rho \bar{\psi}_L \gamma_\rho \psi_L) + \frac{i}{2}(\bar{t}_R \gamma_\rho \partial_\rho t_R - \partial_\rho \bar{t}_R \gamma_\rho t_R) + \\
& + \frac{i}{2}(\bar{b}_R \gamma_\rho \partial_\rho b_R - \partial_\rho \bar{b}_R \gamma_\rho b_R) - \frac{1}{4}W_{\mu\nu}^a W_{\mu\nu}^a - \frac{1}{4}B_{\mu\nu} B_{\mu\nu} - \\
& - \frac{g}{2}\bar{\psi}_L \tau^a \gamma_\rho \psi_L W_\rho^a - \frac{g \tan \theta_W}{6}\bar{\psi}_L \gamma_\rho \psi_L B_\rho - \frac{2g \tan \theta_W}{3}\bar{t}_R \gamma_\rho t_R B_\rho + \\
& + \frac{g \tan \theta_W}{3}\bar{b}_R \gamma_\rho b_R B_\rho; \quad g = \frac{e}{\sin \theta_W}; \\
W_{\mu\nu}^a = & \partial_\mu W_\nu^a - \partial_\nu W_\mu^a + g \epsilon^{abc} W_\mu^b W_\nu^c; \quad B_{\mu\nu} = \partial_\mu B_\nu - \partial_\nu B_\mu.
\end{aligned} \tag{20}$$

Notations here are usual ones and quarks t and b are colour triplets.

Let us look for spontaneous four-fermion interactions

$$\begin{aligned}
& x_1 \bar{\psi}_L^\alpha \gamma_\rho \psi_{L\alpha} \bar{t}_R^\beta \gamma_\rho t_{R\beta}; \quad x_2 \bar{\psi}_L^\alpha \gamma_\rho \psi_{L\alpha} \bar{b}_R^\beta \gamma_\rho b_{R\beta}; \\
& \bar{x}_1 \bar{\psi}_L^\alpha \gamma_\rho \psi_{L\beta} \bar{t}_R^\beta \gamma_\rho t_{R\alpha}; \quad \bar{x}_2 \bar{\psi}_L^\alpha \gamma_\rho \psi_{L\beta} \bar{b}_R^\beta \gamma_\rho b_{R\alpha}; \\
& \frac{y_1}{2} \bar{\psi}_L^{\alpha s} \gamma_\rho \psi_{L\alpha s} \bar{\psi}_L^{\beta r} \gamma_\rho \psi_{L\beta r}; \quad \frac{y_2}{2} \bar{\psi}_L^{\alpha s} \gamma_\rho \psi_{L\alpha r} \bar{\psi}_L^{\beta r} \gamma_\rho \psi_{L\beta s}; \\
& \frac{z_1}{2} \bar{t}_R^\beta \gamma_\rho t_{R\beta} \bar{t}_R^\alpha \gamma_\rho t_{R\alpha}; \quad \frac{z_2}{2} \bar{b}_R^\alpha \gamma_\rho b_{R\alpha} \bar{b}_R^\beta \gamma_\rho b_{R\beta}; \\
& z_{12} \bar{t}_R^\beta \gamma_\rho t_{R\beta} \bar{b}_R^\alpha \gamma_\rho b_{R\alpha}; \quad \bar{z}_{12} \bar{t}_R^\beta \gamma_\rho t_{R\alpha} \bar{b}_R^\alpha \gamma_\rho b_{R\beta}; \\
& \bar{y}_1 = y_2; \quad \bar{y}_2 = y_1; \quad \bar{z}_i = z_i.
\end{aligned} \tag{21}$$

Here α, β are colour indices and s, r are weak isotopic indices. Symbol \bar{a} means interchange of colour summation just in the way as it is done for x_1, x_2 . In the same way, as earlier (5) we introduce dimensionless variables

$$X_i = \frac{x_i \Lambda^2}{16 \pi^2}; \quad Y_i = \frac{y_i \Lambda^2}{16 \pi^2}; \quad Z_i = \frac{z_i \Lambda^2}{16 \pi^2}. \tag{22}$$

From diagram set of equations Fig. 1 we could obtain a complicated set of algebraic equations. Its form is marvelously simplified in the main order of $1/N_c$ expansion. So here we consider just this approximation. Thus for the beginning we get equations for Y_1, Y_2

$$\begin{aligned}
Y_1 = & \frac{N_c}{2} \left(-Y_2^2 - 2Y_1^2 - X_1^2 - X_2^2 - 2Y_1 Y_2 \right); \\
Y_2 = & \frac{N_c}{2} \left(-Y_2^2 - 2Y_1^2 - X_1^2 - X_2^2 - 2Y_1 Y_2 \right).
\end{aligned} \tag{23}$$

This means, that $Y_1 = Y_2 = Y$. For other variables we have

$$\begin{aligned} X_1 &= -N_c (3X_1 Y + 2X_1 Z_1 + X_2 Z_{12}); \\ X_2 &= -N_c (3X_2 Y + 2X_2 Z_2 + X_1 Z_{12}); \\ Y &= -\frac{N_c}{2} (5Y^2 + X_1^2 + X_2^2); \quad \bar{Y} = Y; \quad \bar{Z}_1 = Z_1; \quad \bar{Z}_2 = Z_2; \end{aligned} \quad (24)$$

$$\begin{aligned} Z_1 &= -\frac{N_c}{2} (4Z_1^2 + 2X_1^2 + Z_{12}^2); \quad Z_2 = -\frac{N_c}{2} (4Z_2^2 + 2X_2^2 + Z_{12}^2); \\ Z_{12} &= -2N_c (Z_1 Z_2 + Z_1 Z_{12} + Z_2 Z_{12}); \quad \bar{Z}_{12} = -N_c \bar{Z}_{12}^2. \\ \bar{X}_1 &= -4N_c \bar{X}_1^2; \quad \bar{X}_2 = -4N_c \bar{X}_2^2; \end{aligned} \quad (25)$$

The most important are equations for $\bar{X}_{1,2}$, which we mark separately. If we consider Bethe-Salpeter equations for $\bar{\psi}_L t_R$ and $\bar{\psi}_L b_R$ scalar states again in the main order of $1/N_c$ expansion, we have respectively

$$G_1 = -4N_c \bar{X}_1 F(\xi) G_1; \quad G_2 = -4N_c \bar{X}_2 F(\xi) G_2; \quad \xi = \frac{k^2}{4\Lambda^2}. \quad (26)$$

Here $F(\xi)$ is the same function as earlier (8). This means that in case of a non-trivial solution of one of equations (25) we have zero mass Bogolyubov-Goldstone scalar doublet. Interaction with gauge vector fields according to (20) shifts the level to positive or negative values of the mass squared. Because of the bound state consisting of left and right spinors, only interactions of B -boson enter to diagram Fig. 2. So if $\bar{X}_1 = -1/4N_c$, we have tachyon state with

$$m_0^2 = \frac{g^2 \tan^2 \theta_W}{24\pi^2} \Lambda^2. \quad (27)$$

For other possibility, i.e. $\bar{X}_2 = -1/4N_c$ ($\bar{\psi}_L b_R$ bound state), we have normal sign mass squared

$$m_{Lb}^2 = \frac{g^2 \tan^2 \theta_W}{48\pi^2} \Lambda^2.$$

As we already know, the first possibility leads to Higgs-like symmetry breaking, that is to negative minimum of the effective potential. As for the second case, there is no minima, so here we should take trivial solution $\bar{X}_2 = 0$. It is very important point. Really, we here obtain the explanation of why the t -quark is heavy and the b -quark is light. Only the first possibility corresponds to tachyon and so gives condensate, leading to creation of masses including t -quark mass. The fact is connected with signs of interaction terms in (20). For us here only \bar{X}_1 is important. It is easily seen from set (24) that for all other variables we can take trivial solution $X_1 = X_2 = \dots = 0$.

Next step is normalization of the bound state. Again following previous considerations (13, 14) we have the following normalization condition

$$\frac{N_c G_1^2}{16\pi^2} \log \frac{\Lambda^2}{m^2} = 1; \quad (28)$$

Now we obtain fourfold scalar interaction constant λ

$$\lambda = \frac{N_c G_1^4}{16\pi^2} \log \frac{\Lambda^2}{m^2}. \quad (29)$$

For the moment we have everything for effective Higgs mechanism in our variant of the Standard Model. We immediately come to classical scalar field density η

$$\eta^2 = \frac{m_0^2}{\lambda}; \quad (30)$$

where parameters are uniquely defined (27, 28, 29). We also easily see, that constants of gauge interactions of the scalar doublet are just g for interaction with W and $g' = g \tan \theta_W$ for interaction with B as usually. Now we have at once W , Z and t , b -quark masses

$$M_W = \frac{g \eta}{2}; \quad M_Z = \frac{M_W}{\cos \theta_W}; \quad m_t = \frac{G_1 \eta}{\sqrt{2}}; \quad m_b = 0. \quad (31)$$

Mass of surviving Higgs scalar

$$M_H^2 = 2 m_0^2 = 2 \lambda \eta^2 = \frac{N_c G_1^2 m_t^2}{4 \pi^2} \log \frac{\Lambda^2}{m_t^2}. \quad (32)$$

From (27) we have

$$\Lambda^2 = \frac{3 \pi \cos^2 \theta_W}{\alpha} M_H^2; \quad (33)$$

where as usually α is the fine structure constant. From here and from (32) we have

$$R = \frac{3 G_1^2}{4 \pi^2} \left(\log R + \log \frac{3 \pi \cos^2 \theta_W}{\alpha} \right); \quad R = \frac{M_H^2}{m_t^2}. \quad (34)$$

Now let us discuss phenomenological aspects. We know all masses but that of the Higgs particle. To obtain it let us proceed as follows. From (31) we have

$$G_1 = \frac{g m_t}{\sqrt{2} M_W}; \quad g = \sqrt{\frac{4 \pi \alpha}{\sin^2 \theta_W}} = 0.648; \quad \alpha(M_Z) = \frac{1}{129}. \quad (35)$$

Then for values $m_t = 174 \pm 5 \text{ GeV}$, $M_W = 80.3 \text{ GeV}$ we have $G_1 = 0.993 \pm 0.032$. Substituting this into (34) we have from solution of the equation

$$M_H = 117.1 \pm 7.4 \text{ GeV}. \quad (36)$$

For example, for $m_t = 173 \text{ GeV}$ we obtain $M_H = 115.6 \text{ GeV}$. Result (36) support indications of 115 GeV Higgs [2].

However value $G_1 \simeq 1$ does not fit normalization condition (28). From (28) G_1^2 is rather about 8 than about 1. So we conclude, that condition (28) contradicts to the observed t -quark mass. We would emphasize, that the normalization condition is the only flexible point in our approach. The next section will be devoted to discussion of this problem.

3 Normalization condition

Scalar bound state in our approach consists of anti-doublet (t_L, b_L) and singlet t_R . It evidently has weak isotopic spin 1/2. Let us denote its field as ϕ

$$\phi = (\bar{b}_L t_R \quad \bar{t}_L t_R); \quad \phi^+ = (\bar{t}_R b_L \quad \bar{t}_R t_L). \quad (37)$$

From the previous results we have the following terms in the effective Lagrangian

$$\begin{aligned} N \frac{\partial \phi^+}{\partial x^\mu} \frac{\partial \phi}{\partial x^\mu} + m_0^2 \phi^+ \phi - \Lambda (\phi^+ \phi)^2; \\ N = \frac{N_c G_1^2}{16 \pi^2} \log \frac{\Lambda^2}{m^2}; \end{aligned} \quad (38)$$

where parameters are defined in (27, 29). As for normalization parameter N , it does not satisfy us. So we may study a possibility of quasi-averages effect for ϕ interactions, which can change a coefficient afore the kinetic term. So, let us consider the following possible interactions in addition to (38)

$$L_{int}(W) = \frac{\xi_{01}}{2} \frac{\partial \phi^+}{\partial x^\mu} \frac{\partial \phi}{\partial x^\nu} W_{\mu\rho}^a W_{\nu\rho}^a + \frac{\eta_{01}}{2} \frac{\partial \phi^+}{\partial x^\mu} \frac{\partial \phi}{\partial x^\mu} W_{\nu\rho}^a W_{\nu\rho}^a; \quad (39)$$

$$L_{int}(B) = \frac{\xi_{00}}{2} \frac{\partial \phi^+}{\partial x^\mu} \frac{\partial \phi}{\partial x^\nu} B_{\mu\rho} B_{\nu\rho} + \frac{\eta_{00}}{2} \frac{\partial \phi^+}{\partial x^\mu} \frac{\partial \phi}{\partial x^\mu} B_{\nu\rho} B_{\nu\rho}. \quad (40)$$

In obtaining compensation equations we take into account possibility of triple W gauge bosons coupling, which was discussed in various papers (e.g. [13]) and, in particular, in a variant of dynamical breaking of the electroweak symmetry, which the author considered some time ago [11].

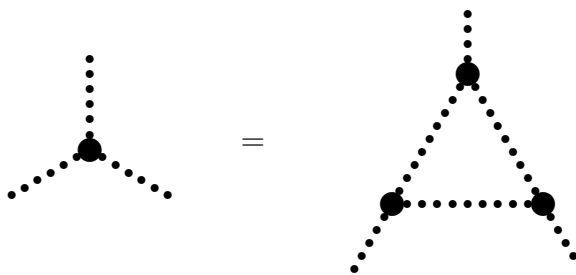


Figure 3. Diagram equation for triple gauge constant λ_V .

In this variant the Bogolyubov quasi-averages method is applied to possible origin of the triple interaction

$$\frac{g\lambda_V}{M_W^2} \epsilon_{abc} W_{\mu\nu}^a W_{\nu\rho}^b W_{\rho\mu}^c; \quad (41)$$

and corresponding one-loop compensation equation looks like (see Fig. 3)

$$\lambda_V = \lambda_V \left(\frac{g\lambda_V}{M_W^2} \right)^2 \frac{\Lambda^4}{128 \pi^2}; \quad (42)$$

We have solutions of this equation: trivial one $\lambda_V = 0$ and two non-trivial ones

$$\lambda_V = \pm \lambda_0; \quad \lambda_0 = \frac{8\sqrt{2} M_W^2}{g \Lambda^2}. \quad (43)$$

In the following we assume, that genuine value of λ_V may differ from value (43) in the range of 15-20%.

Set of equations in one-loop approximation according to diagrams presented at Fig. 4 looks like

$$\begin{aligned} \xi_1 &= -\frac{1}{3}\xi_1^2 - \frac{1}{3}\xi_1\eta_1 - \frac{1}{12}\eta_1^2 + \frac{4}{3}\zeta\xi_1; \\ \eta_1 &= -\frac{1}{48}\xi_1^2 - \frac{1}{12}\xi_1\eta_1 - \frac{1}{12}\eta_1^2 + 4\zeta\left(\frac{5}{6}\xi_1 + 2\eta_1\right); \end{aligned} \quad (44)$$

$$\xi_0 = -\frac{1}{3}\xi_0^2 - \frac{1}{3}\xi_0\eta_0 - \frac{1}{12}\eta_0^2; \quad (45)$$

$$\eta_0 = -\frac{1}{48}\xi_0^2 - \frac{1}{12}\xi_0\eta_0 - \frac{1}{12}\eta_0^2;$$

$$\xi_1 = \frac{\Lambda^4}{16\pi^2}\xi_{01}; \quad \eta_1 = \frac{\Lambda^4}{16\pi^2}\eta_{01}; \quad \zeta = \left(\frac{\lambda_V}{\lambda_0}\right)^2.$$

$$\xi_0 = \frac{\Lambda^4}{16\pi^2}\xi_{00}; \quad \eta_0 = \frac{\Lambda^4}{16\pi^2}\eta_{00}.$$

For parameters describing interaction of vector singlet B there is no contribution of the triple vertex (41), because B is an Abelian field.

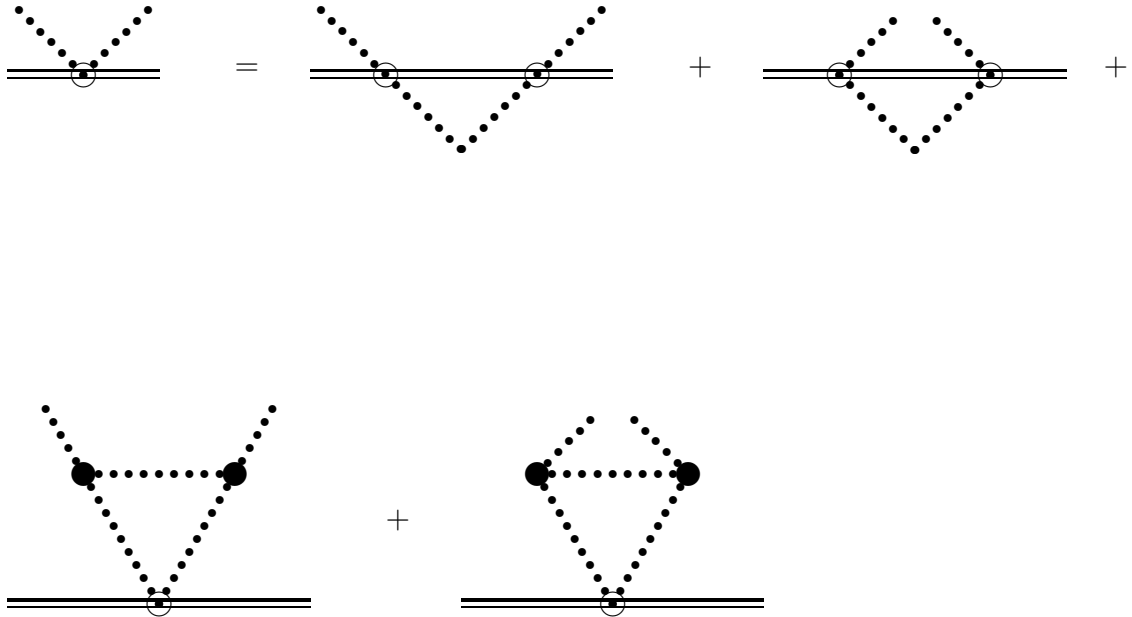


Figure 4. Diagrams representing equations for $\phi^+ \phi WW$ vertices.

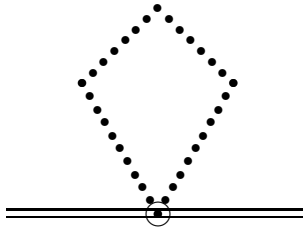


Figure 5. Diagram for contribution of $\phi^+ \phi WW$ vertices to the normalization condition.

Parameters ξ_i, η_i enter into normalization condition according to account of diagram Fig 5. Now this condition takes the form

$$\frac{N_c G_1^2}{16 \pi^2} \log \frac{\Lambda^2}{m^2} + \frac{9}{4} (\xi_1 + 2\eta_1) + \frac{3}{4} (\xi_0 + 2\eta_0) = 1; \quad (46)$$

From this expression we obtain

$$G_1^2 = \frac{(4 - 9(\xi_1 + 2\eta_1) - 3(\xi_0 + 2\eta_0)) 4 \pi^2}{3 (\log(3 \pi \cos^2 \theta_W M_H^2) - \log(\alpha m_t^2))}. \quad (47)$$

We take M_H (36) and obtain results, which are presented at Table 1.

Table 1.
Yukawa coupling G_1 and the t -quark mass
in dependence on λ_V .

ζ	ξ_1	η_1	G_1	λ_V	$m_t \text{ GeV}$	$G_1(\xi_0, \eta_0 \neq 0)$
1	1.723	- 0.820	2.67	- 0.0286	467.8	5.31
1.2	3.056	- 1.421	2.13	- 0.0313	373.2	5.31
1.4	4.371	- 1.999	1.195	- 0.0338	209.4	4.75
1.42	4.502	- 2.056	1.047	- 0.0341	183.4	4.71
1.422	4.515	- 2.062	1.031	- 0.0341	180.6	4.71
1.424	4.528	- 2.068	1.015	- 0.0341	177.8	4.70
1.426	4.541	- 2.073	0.998	- 0.0342	174.8	4.70
1.428	4.554	- 2.079	0.982	- 0.0342	172.0	4.70
1.43	4.567	- 2.085	0.964	- 0.0342	168.9	4.69
0	- 2.781	- 0.215	8.392	0	1470.7	
0	0	0	2.927	0	512.8	

Table 1 contains results of calculations for the case of trivial solution of set (45), i.e $\xi_0 = \eta_0 = 0$ (all columns but the last); this last column presents results for nontrivial solution of set (45): $\xi_0 = -2.781, \eta_0 = -0.215$.

What are criteria for choosing a solution? The main criterion is provided by an energy density of a vacuum. We know, that in case of appearance of scalar Higgs condensate η the vacuum energy density reads

$$E = - \frac{m_0^4}{4 \lambda}; \quad (48)$$

where parameters are defined in (27), (29). We see, that λ is proportional to G_1^4 , thus the smaller is G_1 and consequently m_t , the deeper becomes the energy density minimum. Therefore we have to choose the solution, which leads to the minimal value of m_t .

From Table 1 we see, that for calculated value $\lambda_V = -\lambda_0$ we have minimal m_t in comparison with two last lines. The last line but one corresponds to non-trivial solution with $\lambda_V = 0$ and the last line give results for completely trivial solution ($\Lambda = \xi = \eta = 0$). Both ones give larger values for m_t and thus are not suitable. The last column of the table also corresponds to non-minimal values of G_1 and thus the corresponding solutions are unstable.

However, $m_t \simeq 470 \text{ GeV}$ is too large, so let us look for values of $\zeta = (\lambda_V/\lambda_0)^2$, which give realistic values of the t -quark mass. Namely, values $\zeta \simeq 1.42 \div 1.43$, ($\lambda_V = -0.0342$) give G_1 to be just in correspondence with relation (35). So, contradiction of the normalization condition with value of the t -quark mass is removed. Thus we come to the conclusion, that we may not take into account of the normalization condition in considering estimates of composite Higgs mass, as it is done in the previous section.

How we can interpret the situation, when the desirable value for λ_V is about 20% larger, than the calculated one? We would state, that corrections to the leading approximation, which is used here, might be just of this order of magnitude. To estimate the effect of correction let us consider contribution of usual electroweak triple W vertex

$$V_{\mu\nu\rho}(p, q, k) = g \left(g_{\mu\nu}(q_\rho - p_\rho) + g_{\nu\rho}(k_\mu - q_\mu) + g_{\rho\mu}(p_\nu - k_\nu) \right);$$

(where p, q, k and μ, ν, ρ are as usually incoming momenta and indices of W s) to compensation equation (42), which defines λ_V . In addition to diagram Fig. 3 we take three diagrams, in which one of vertices is changed to $V_{\mu\nu\rho}$. We have to add also contribution of four- W vertex, which is contained in triple vertex (41). This contribution restores the gauge invariance of the result. Thus we obtain a contribution, which is proportional to g/π . Namely, instead of (42) we now have

$$\lambda_V = \lambda_V \left(\left(\frac{g\lambda_V}{M_W^2} \right)^2 \frac{\Lambda^4}{128\pi^2} + \frac{3g}{16\pi^2} \frac{g\lambda_V\Lambda^2}{M_W^2} \right);$$

That is, if $\lambda_V \neq 0$

$$1 = \left(\frac{\lambda_V}{\lambda_0} \right)^2 + \frac{3g}{\sqrt{2}\pi} \frac{\lambda_V}{\lambda_0}; \quad (49)$$

and from (49) we have

$$\lambda_V \simeq \lambda_0 \left(\pm 1 - \frac{3g}{2\sqrt{2}\pi} \right). \quad (50)$$

Value of g (35) gives the correction term here to be about 20%, what corresponds to data presented in Table 1. We consider result (50) as qualitative argument for possibility of consistent description of data in the framework of our approach. Full study of this problem needs special efforts. So for the moment one may only state, that value

$$\lambda_V \simeq -0.034; \quad (51)$$

which excellently fits t -quark mass, is possible in the approach being considered here. Sign of λ_V is chosen due to experimental limitations $\lambda_V = -0.037 \pm 0.030$ [14]. We

see, that our result (51) fits this restriction quite nicely. We consider this result (51) as a prediction for triple gauge coupling.

We have no proof that the possibility being discussed here is the only one, which can improve situation with the normalization condition. However all other possibilities, which were considered in the course of performing the work, lead to wrong sign of corresponding contributions to this condition. That is t -quark mass becomes even larger, than 513 GeV . So we are inclined to consider this possibility, especially prediction (51) as quite promising. In any case we have an example of a variant, which has no contradiction with all what we know.

4 Muon g-2

Let us start with anomalous triple gauge coupling (41) and consider possible additional interactions of composite Higgs with charged and neutral W -s

$$f_{ch} HW_{\mu\nu}^* W_{\mu\nu}; \quad f_0 HW_{\mu\nu}^0 W_{\mu\nu}^0. \quad (52)$$

Let us consider at first "zero" values of parameters f_i , which are defined by interactions already introduced above.

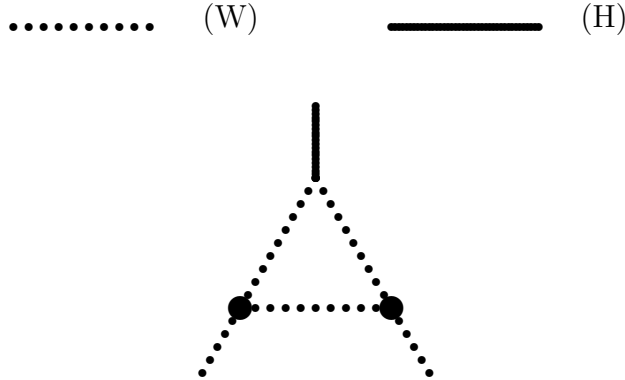


Figure 6. Diagram for zero approximation of HWW interactions.

From one-loop diagram Fig. 6 we have corresponding vertices

$$V_i^0 = f_i^0 (g_{\mu\nu}(k q) - k_\nu q_\mu);$$

where

$$\begin{aligned} f_0^0 &= \frac{g M_W}{8\pi^2} \left(\frac{g \lambda_V}{M_W^2} \right)^2 \Lambda^2; \\ f_{ch}^0 &= \frac{2 g M_W}{8\pi^2} \left(\frac{g \lambda_V}{M_W^2} \right)^2 \Lambda^2; \end{aligned} \quad (53)$$

Here k , q , μ , ν are respectfully momenta and indices of W -s. Other parameters are defined above. Diagrams Fig. 7 with use of numbers (53) gives contribution to muon $(g - 2)$ of

order of magintude $\simeq 2 \cdot 10^{-10}$, that is too small in comparison with experimental data [3] $(43 \pm 16) \cdot 10^{-10}$.

Let us consider one-loop equation in quasi-averages method. The corresponding compensation equation, presented at Fig. 8, reads

$$f_i = f_i^0 + \frac{\Lambda^2}{32\pi^2} f_i^3. \quad (54)$$

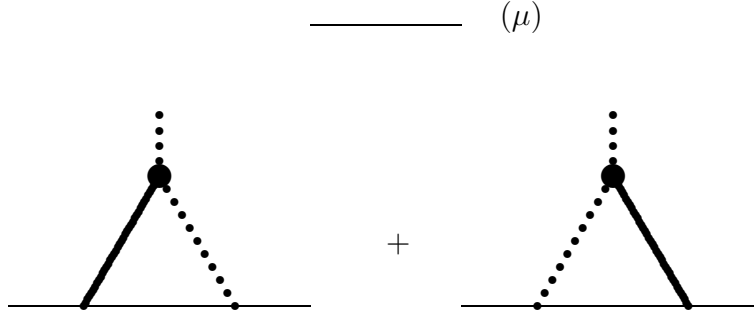


Figure 7. Diagrams for HW^0W^0 contribution to the muon anomalous magnetic moment.

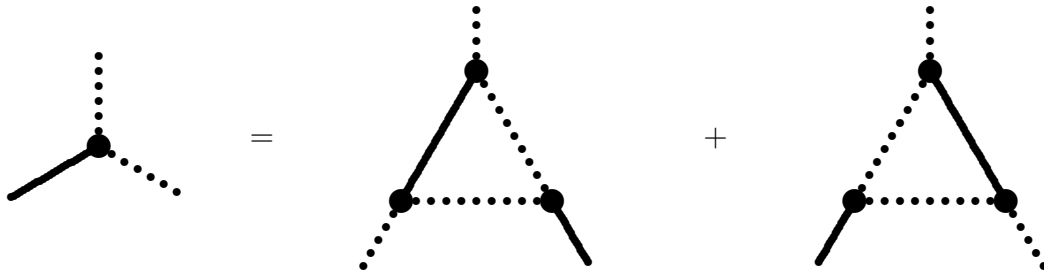


Figure 8. Diagram representation of equations for f_i in the quasi-averages method.

Here f_i^0 are quite small, so there are three solutions

$$f_{i,1} = f_i^0; \quad f_{i,(2,3)} = \pm \frac{4\sqrt{2}\pi}{\Lambda}. \quad (55)$$

For solutions $f_{0,(2,3)}$ we have again from diagrams Fig. 7

$$\Delta a = \pm \frac{-\sqrt{2}g m_\mu^2}{16\pi\Lambda M_W} \left(\ln \frac{\Lambda^2}{M_H^2} - \frac{(1 - 4\sin^2\theta_W)M_Z^2}{M_H^2 - M_Z^2} \ln \frac{M_H^2}{M_Z^2} \right). \quad (56)$$

Substituting into (56)

$$g = 0.653; \quad M_H = 115 \text{ GeV}; \quad \Lambda = \frac{2\sqrt{3}\pi M_H}{g \tan\theta_W} = 3506 \text{ GeV};$$

and usual values for m_μ , M_W , we have

$$\Delta a = \pm (-49.4 \cdot 10^{-10}). \quad (57)$$

The agreement is obvious (for sign minus in (55)).

In other notations we have

$$\begin{aligned} \Delta a = \pm \frac{-\alpha m_\mu^2}{4\sqrt{6}\pi \sin \theta_W \cos \theta_W M_H M_W} & \left(\ln \frac{3\pi \cos^2 \theta_W}{\alpha} - \right. \\ & \left. - \frac{(1-4\sin^2 \theta_W)M_Z^2}{M_H^2 - M_Z^2} \ln \frac{M_H^2}{M_Z^2} \right); \end{aligned} \quad (58)$$

From here we may reformulate the result in other way. Let us take data [3] and define M_H . We have for overall sign plus

$$M_H = 132^{+78}_{-37}; \quad (59)$$

Sign in Eq. (55) is an important point. It is defined by stability condition, which is already used in Section 3. Remind, that the larger is $|\lambda_V|$ the more stable is the solution and vice versa. Now, let us consider contributions to the compensation equation (42) for λ_V . According to diagrams containing vertices (52) we have instead of (42)

$$\lambda_V = \lambda_V \frac{f_{ch}(f_{ch} + f_0) \Lambda^2}{32\pi^2} + \frac{\lambda_V}{128\pi^2} \left(\frac{g\lambda_V \Lambda^2}{M_W^2} \right)^2. \quad (60)$$

In view of (55) we have $f_0 = \pm f_{ch}$ for nontrivial solutions for both f_i . For plus sign we have positively definite first term in the rhs. of (60). Substituting nontrivial solution (55) we come to coefficient 2 afore the λ_V term in the rhs., and thus there is no nontrivial solution of the equation at all. So we have $\lambda_V = 0$, that corresponds to unstable situation. For minus sign the contribution vanishes and one have to consider next approximations. The same is valid for trivial charged solution $f_{ch} = 0$. For the last case the next terms are defined by contributions of one-loop diagrams Fig. 9, in which the upper line corresponds to neutral gauge boson. We would draw attention to the fact, that interaction vertex HW^+W^- is the usual one. Thus we have

$$\begin{aligned} \lambda_V &= \lambda_V \frac{g M_W f_0}{48\pi^2} \ln \frac{\Lambda^2}{M_H^2} + \lambda_V \left(\frac{g\lambda_V}{M_W^2} \right) \frac{\Lambda^4}{128\pi^2} = \\ &= \pm \lambda_V \frac{\sqrt{2} g M_W}{12\pi\Lambda} \ln \frac{\Lambda^2}{M_H^2} + \lambda_V \left(\frac{g\lambda_V}{M_W^2} \right) \frac{\Lambda^4}{128\pi^2}. \end{aligned} \quad (61)$$

This means, that just for minus sign of f_0 nontrivial solution for $|\lambda_V|$ becomes larger, and thus, according to discussion in Section 3 with the use of Table 1, the minimum becomes deeper.

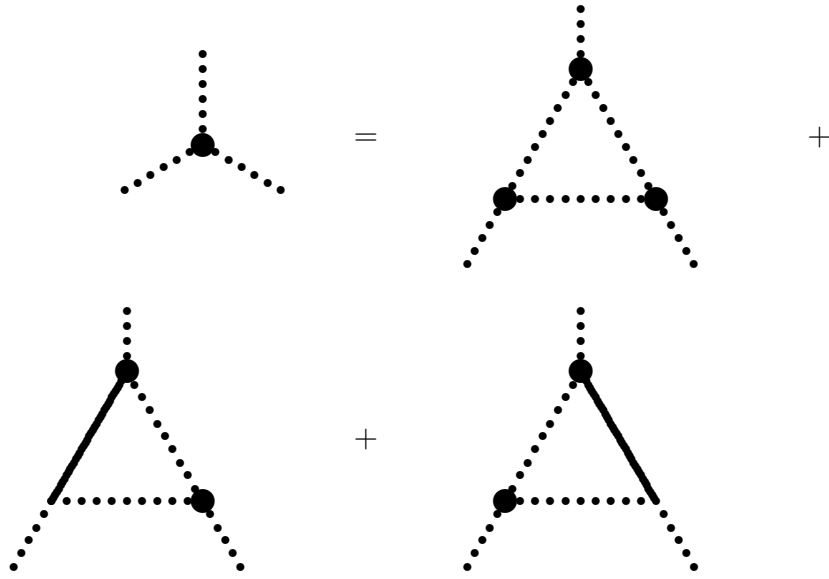


Figure 9. contributions of f_0 to equation for λ_V .

We easily see, that for possibility $f_{ch} = -f_0$ the contribution becomes smaller in absolute value because due to opposite signs of f_0 and f_{ch} their contributions almost cancel. Thus this case corresponds to the less deep minimum. We come to the conclusion, that the most stable solution corresponds to

$$f_{ch} = 0; \quad f_0 = -\frac{4\sqrt{2}\pi}{\Lambda}; \quad \Delta a = 49.4 \cdot 10^{-10}. \quad (62)$$

So we obtain the result, that our approach chooses minus sign of (55) and this means plus sign in Eqs. (56, 58) in full correspondence with experimental indications [3].

Finally, we have the following vertices of Higgs particle H with gauge bosons Z, A

$$\begin{aligned} H A A : & - \sin^2 \theta_W \frac{4\sqrt{2}\pi}{\Lambda} (g_{\mu\nu}(k q) - k_\nu q_\mu); \\ H Z A : & - \sin \theta_W \cos \theta_W \frac{4\sqrt{2}\pi}{\Lambda} (g_{\mu\nu}(k q) - k_\nu q_\mu); \\ H Z Z : & \frac{g M_W}{\cos^2 \theta_W} g_{\mu\nu} - \cos^2 \theta_W \frac{4\sqrt{2}\pi}{\Lambda} (g_{\mu\nu}(k q) - k_\nu q_\mu); \end{aligned} \quad (63)$$

where k, q, μ, ν are respectfully momenta and indices of gauge bosons.

Now, interactions (63) radically change branching ratios of H decays. For $M_H = 115 \text{ GeV}$ we present results at Table 2.

Interactions (63) lead also to a change in predictions for Higgs production. For e^+e^- reactions we present results of calculations for three energies: 189 GeV, 207 GeV (maximal luminosity at LEP2) and 250 GeV (to demonstrate future possibilities). In calculations ISR is taken into account. The results are presented in Table 3.

Table 2.
Branching ratios for 115 GeV Higgs decays
in the present model (new)
and in Standard Model (SM).

decay channel	B.R. new %	B.R. SM %
$H \rightarrow \gamma\gamma$	62.8	0.3
$H \rightarrow \gamma Z$	22.3	0.1
$H \rightarrow b\bar{b}$	11.7	79.9
$H \rightarrow \tau\bar{\tau}$	1.6	9.3
$H \rightarrow c\bar{c}$	0.4	2.5
$H \rightarrow g g$	0.1	0.9
$H \rightarrow W^*W^*$	0.9	6.0
$H \rightarrow Z^*Z^*$	0.2	1.0

Table 3.
Cross-sections (pb) of Higgs production reactions
for three different energies in the present
model (new) and in Standard Model (SM).

reaction	189 GeV	207 GeV	250 GeV
$e^+e^- \rightarrow HZ$ new	0.000	0.300	1.997
$e^+e^- \rightarrow HZ$ SM	0.000	0.057	0.273
$e^+e^- \rightarrow H\gamma$ new	0.124	0.157	0.217
$e^+e^- \rightarrow H\gamma$ SM	0.000	0.000	0.000
$e^+e^- \rightarrow e^+e^- H$ new	0.059	0.080	0.180
$e^+e^- \rightarrow e^+e^- H$ SM	0.000	0.002	0.010
$e^+e^- \rightarrow H + X$ (total) new	0.18	0.54	2.39
$e^+e^- \rightarrow H + X$ (total) SM	0.00	0.06	0.28

We see from Tables 2 and 3, that for real search [2] of Higgs in the channel $H \rightarrow b\bar{b}$, $\sigma \cdot B.R$ are 0.035 pb (new) and 0.046 pb (SM) that means almost the same. By the way, the 25% decrease of the new result in comparison with SM prediction may serve for an explanation of rather indefinite evidence [2] for 115 GeV Higgs. However, in the channel $H \rightarrow \gamma\gamma$ there is very considerable effect. For $\sqrt{s} = 189\text{ GeV}$, where there are data [15], [16] $\sigma(e^+e^- \rightarrow H\gamma) \cdot BR(H \rightarrow 2\gamma) < 0.122\text{ pb}$ for $M_H \simeq 110\text{ GeV}$ to be compared with our prediction $\sigma(H\gamma) \cdot BR(2\gamma) = 0.078\text{ pb}$. So, there is no contradiction with data. For $\sqrt{s} = 207\text{ GeV}$ we predict $\sigma(H\gamma) \cdot BR(2\gamma) = 0.099\text{ pb}$ that means e.g. around 14 events in the already collected L3 data. So it seems advisable to develop these data and look for channel $e^+e^- \rightarrow 3\gamma$, two of the photons being due to decay $H \rightarrow \gamma\gamma$.

We calculate also effect of the model for Higgs production at FNAL. Corresponding cross-sections are presented at Table 4. We see a considerable enhancement of the production process in our model. Thus a check of the model at FNAL might be possible provided integral luminosity being few tens of pb^{-1} .

Table 4.

Cross-sections of Higgs production in $p\bar{p}$ reactions
 at $\sqrt{s} = 2000 \text{ GeV}$ in the present model (new)
 and in Standard Model (SM).

reaction	$\sigma \text{ pb new}$	$\sigma \text{ pb SM}$
$p\bar{p} \rightarrow H Z + X$	0.97	0.10
$p\bar{p} \rightarrow H W^\pm + X$	0.17	0.17
$p\bar{p} \rightarrow H \gamma + X$	0.17	0.00
$p\bar{p} \rightarrow p\bar{p} H + X$	0.35	0.08
$p\bar{p} \rightarrow H + X$ (total)	1.66	0.35

Note, that the enhancement of production processes is connected with the negative sign in main quantity f_0 (55). For the positive sign we have just the opposite situation of suppression of H production. In this case one cannot even interpret the indications for 115 GeV Higgs [2]. So once more we would emphasize the importance of this sign definition, which in our model follows from the basic property of stability of a scalar condensation.

5 Discussion

Thus as a result of our study of the model we now come to the theory, which describe Standard electroweak interaction of:

1. gauge vector bosons sector with input of constants g and θ_W ;
2. heavy quark doublet t, b with the t -quark mass $174 \pm 5 \text{ GeV}$ and the b mass zero;
3. necessary composite Higgs sector with mass of surviving neutral scalar particle $M_H = 117 \pm 7 \text{ GeV}$.

In addition to these standard interactions there are also extra effective interactions, which act in momentum regions limited by effective cut-off $\Lambda \simeq 3500 \text{ GeV}$. We calculate the last number e.g. from relation (27). Three parameters (g, θ_W, Λ) are the only fundamental input of the model. As a technical input we consider triple gauge constant λ_V , which in range of 20% agrees with the calculated value (43), but its precise value is defined by the next approximations. We emphasize, that the presence of such interaction with constant (51) in the framework of the model is necessary. We consider result (51) as very important prediction of the model. Of course, the most important for the model is the prediction, that hints for 115 GeV Higgs [2] have to be confirmed. We also would emphasize the importance of prediction for new contribution to the muon anomalous magnetic moment Δa (62), which agrees with experimental data. Of course, the experimental status of the effect is not yet decisive and needs further clarification. Arguments are expressed repeatedly, that uncertainties in hadronic contributions to $g - 2$ do not allow to insist on discrepancy with SM (see, e.g. [17]). However, the result being obtained here does not contradict to any calculation of the effect, including that of [17].

It is worthwhile here to comment the problem of accuracy of the approach. Our approximations are the following.

1. One-loop diagrams. We estimate accuracy to be around $\bar{X}_1 \simeq 0.08$.
2. Corrections being of order of magnitude g/π give uncertainty around 0.2.

3. The leading order of $1/N_c$ expansion. Usually precision of $1/N_c$ expansion is estimated to be $1/N_c^2 \simeq 0.11$.

4. We keep only logarithmic terms. Uncertainty is estimated to be $1/\log(\Lambda^2/m_t^2) \simeq 0.16$.

Thus the combined accuracy, provided items 1 – 4 being independent, is estimated to be around 29%. As a matter of fact, all uncertainties, which we have encountered above fit into this range.

For the moment we have only one quark doublet. Remind, that now we understand why the t -quark is heavy and the b -quark is almost massless. We consider heavy t, b doublet as the most fundamental one in the sense, that it defines the main part of heavy particles masses. Indeed, composite Higgs scalars are just consisting of these quarks. We may immediately introduce all other quarks and leptons with zero mass completely in the line prescribed by the Standard Model. So at this stage of study of the model we deal with massive W, Z, t, H and massless all other particles. We may expect, that masses of quarks and leptons will appear in subsequent approximations. We have to expect their value to be less than 29% of our heavy masses, that is $m_i \leq 23 \text{ GeV}$. All the masses known satisfy this restriction. We could expect also, that in subsequent approximations Higgs scalars are not composed of only heavy quarks, but have admixture of lighter quarks and leptons.

Additional contact interactions (21) include four-fermion interactions of heavy quarks t, b . So, there is practically no experimental limitations on the corresponding coupling constant. Limitations exist only for contact interactions of light quarks. Limitations for triple gauge interaction (41) were mentioned above and were shown to agree with predicted value (51).

Experimental consequences of interactions (52) are discussed above and shown to have no contradiction with the present data.

To conclude the author would state, that the variant being studied presents a possibility to formulate realistic electroweak interaction without elementary scalars, which are substituted by composite effective scalar fields. The dynamics of the variant is defined in the framework of the Bogolyubov quasi-averages method. Consequences of the approach contains no contradiction with the existing data and agree with two would-be effects: 115 GeV Higgs indications and evidence for deviation from SM prediction in muon $g - 2$. Definite predictions make checks of the variant to be quite straightforward.

Appendix

Let us consider a theory with combination of four-fermion interactions (3). We take the simplest nontrivial term in the Bethe-Salpeter equation for connected four-fermion amplitude, corresponding to Lorentz structure $\bar{\psi}_L \gamma_\rho \psi_L \bar{\psi}_R \gamma_\rho \psi_R = -2 \bar{\psi}_L \psi_R \bar{\psi}_R \psi_L$, which is presented at Fig. 10.

The kernel for this equation corresponds to simple loop, which gives the following expression

$$K(p, q) = i \frac{3x(y+z)}{16\pi^2} (p-q)^2 \log(p-q)^2 + \text{const} + \mathcal{O}((p-q)^2). \quad (64)$$

We are interested in momentum dependence, so we consider just the logarithmic term in the kernel, i.e. the first term in Eq. (64), which we denote $K_{\log}(p, q)$. We shall see below,

that terms containing $const$ and $const(p - q)^2$ give zero contribution due to boundary conditions. Equation for four-fermion amplitude $F(p)$, corresponding to Fig. 10, looks like (after applying of Wick rotation)

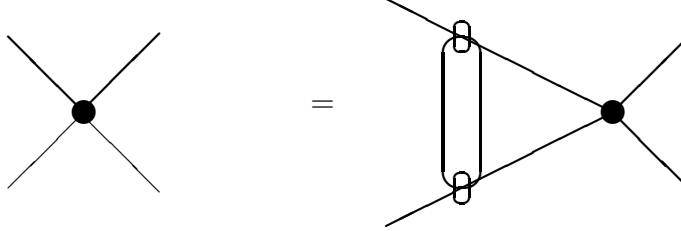


Figure 10. Bethe-Salpeter equation in quasi-ladder approximation.

$$F(p) = -i \int \frac{K_{log}(p, q) F(q)}{q^2} d^4 q = \beta \int \frac{(p - q)^2 \log(p - q)^2 F(q)}{q^2} d^4 q; \quad (65)$$

$$\beta = \frac{3x(y + z)}{16\pi^2}.$$

Equations of such type can be studied in the same way as more simple equations with kernels being proportional to $((p - q)^2)^{-1}$. The method to solve the latter ones was known a long time ago [18]. For logarithmic case basic angular integrals are the following

$$\int d\Omega_4 \log(p - q)^2 = \pi^2 \left(\theta(x - y) \left(\frac{y}{x} + 2 \log x \right) + \theta(y - x) \left(\frac{x}{y} + 2 \log y \right) \right);$$

$$\int d\Omega_4 (p q) \log(p - q)^2 = \frac{\pi^2}{3} \left(\theta(x - y) \left(\frac{y^2}{x} - 3y \right) + \theta(y - x) \left(\frac{x^2}{y} - 3x \right) \right); \quad (66)$$

$$x = p^2, \quad y = q^2.$$

Integrals (66) are sufficient for angular integrations in equation (65). So we have

$$F(x) = \frac{\beta}{32\pi^2} \left(\frac{1}{3x} \int_0^x y^2 F(y) dy + 3 \int_0^x y F(y) dy + 2 \log x \int_0^x y F(y) dy + \right. \\ \left. + 2x \log x \int_0^x F(y) dy + 2 \int_x^\infty y \log y F(y) dy + x \int_x^\infty (3 + 2 \log y) F(y) dy + \right. \\ \left. + \frac{x^2}{3} \int_x^\infty \frac{F(y)}{y} dy \right). \quad (67)$$

Applying differentiations in proper order, we obtain differential equation

$$\frac{d^3}{dx^3} \left(x^2 \frac{d^3}{dx^3} (x F(x)) \right) = -\frac{\beta}{8\pi^2} \frac{F(x)}{x}. \quad (68)$$

Eq. (68) is easily transformed to the canonical form of Meijer equation [19]

$$\left(y \frac{d}{dy} + \frac{1}{2} \right) \left(y \frac{d}{dy} \right) \left(y \frac{d}{dy} \right) \left(y \frac{d}{dy} - \frac{1}{2} \right) \left(y \frac{d}{dy} - \frac{1}{2} \right) \left(y \frac{d}{dy} - 1 \right) F(y) + \\ + y F(y) = 0; \quad y = \frac{\beta}{512\pi^2} x^2. \quad (69)$$

Equation (68) (or (69)) is equivalent to integral equation (67) provided proper boundary conditions be fulfilled. The first one is connected with convergence of integrals at infinity. The most intricate conditions are connected with behaviour at $x \rightarrow 0$. From Eq. (69) we see, that at zero there are the following independent asymptotics:

$$\frac{a_{-1}}{x}, a_{0l} \log x, a_0, a_{1l} x \log x, a_1 x, a_2 x^2. \quad (70)$$

To obtain conditions for a_i one has to substitute into Eq. (67)

$$F(y) = -\frac{8\pi^2}{\beta} x \frac{d^3}{dx^3} \left(x^2 \frac{d^3}{dx^3} (x F(x)) \right);$$

and perform integrations by parts. Thus we come to conditions

$$a_{-1} = a_{0l} = a_{1l} = 0. \quad (71)$$

These results, in particular, lead to zero values of integrals

$$\int_0^\infty F(y) dy = \int_0^\infty y F(y) dy = 0;$$

that guarantees the absence of contributions of constant terms in the initial equation, which we have mentioned above.

According to properties of Meijer functions [19] we have unique solution of Eq. (69) with the boundary conditions (71)

$$F(x) = \frac{\sqrt{\pi}}{2} G_{06}^{30} \left(y \mid 0, \frac{1}{2}, 1; -\frac{1}{2}, 0, \frac{1}{2} \right); \quad y = \frac{\beta}{512\pi^2} x^2. \quad (72)$$

This function has all qualities of a form-factor. It is equal to unity at the origin and decreases with oscillations at infinity. Effective cut-off is estimated from (72)

$$\Lambda^2 = \frac{16\sqrt{2}\pi}{\sqrt{\beta}}. \quad (73)$$

Thus we demonstrate how the effective cut-off arises. Of course, it is done in the quasi-ladder approximation, but we think, that an account of non-linearities changes numbers, but does not change the situation qualitatively. In the present work we will not go further and will not try to connect these considerations with realistic numbers.

References

- [1] P.W. Higgs, Phys. Lett. **12**, 132 (1964); Phys. Rev. Lett. **13**, 508 (1964); Phys. Rev. **145**, 1156 (1966).
- [2] R. Barate et al. (the ALEPH Collaboration), Phys. Lett. B **495**, 1 (2000); M. Acciarri et al. (the L3 Collaboration), Phys. Lett. B **495**, 18 (2000).
- [3] H.B. Brown (Brookhaven E821 Collaboration), Phys. Rev. Lett. **86** 2227 (2001).

- [4] B.A. Arbuzov, hep-ph/0005032.
- [5] B.A. Arbuzov, hep-ph/0102311.
- [6] N.N. Bogolyubov, Preprint JINR D-781, Dubna (1961).
- [7] B.A. Arbuzov, A.N. Tavkhelidze and R.N. Faustov, Doklady Acad. Nauk SSSR (Sov. Phys. Doklady) **139**, 345 (1961).
- [8] N.N. Bogolyubov, *Physica* **26**, Suppl. 1 (1960).
- [9] E.S. Fradkin, Trudy FIAN SSSR (Lebedev Institute Proceedings) **29**, 7 (1965).
- [10] J. Goldstone, *Nuovo Cimento* **19**, 154 (1961).
- [11] B.A. Arbuzov, *Phys. Lett. B* **288**, 179 (1992).
- [12] H. Terazawa, Y. Chikashige and K. Akama, *Phys. Rev. D* **15**, 480 (1977).
- [13] K. Hagiwara, R.D. Peccei, D. Zeppenfeld and K. Hikasa, *Nucl. Phys. B* **282**, 253 (1987).
- [14] A. Hurtu, Precision tests of the electroweak gauge theory, Rapporteur talk at the XXXth International Conference on High Energy Physics, July 27 – August 2, 2000, Osaka, Japan, to be published.
- [15] M. Acciarri et al. (the L3 Collaboration), *Phys. Lett. B* **475**, 198 (2000).
- [16] M. Acciarri et al. (the L3 Collaboration), *Phys. Lett. B* **489**, 102 (2000).
- [17] A.A. Pivovarov, hep-ph/0110248.
- [18] B.A. Arbuzov and A.T. Filippov, *Nuovo Cimento* **38**, 796 (1965).
- [19] H. Bateman and A. Erdelyi, Higher transcendental functions, vol. 1, New York, Toronto, London, McGraw-Hill, 1953.